Published OnlineFirst September 7, 2012; DOI:10.1158/2159-8290.CD-12-0103

CANCER DISCOVERY

Reactivation of ERK Signaling Causes Resistance to EGFR Kinase Inhibitors

Dalia Ercan, Chunxiao Xu, Masahiko Yanagita, et al.

Cancer Discovery 2012;2:934-947. Published OnlineFirst September 7, 2012.

Published OnlineFirst September 7, 2012; DOI:10.1158/2159-8290.CD-12-0103

RESEARCH ARTICLE

Reactivation of ERK Signaling Causes Resistance to EGFR Kinase Inhibitors

Dalia Ercan[1,2], Chunxiao Xu[1,3], Masahiko Yanagita[1,3], Calixte S. Monast[11], Christine A. Pratilas[12,14], Joan Montero[3], Mohit Butaney[1,3], Takeshi Shimamura[1,3,15], Lynette Sholl[8], Elena V. Ivanova[5], Madhavi Tadi[12,14], Andrew Rogers[1,3], Claire Repellin[1,3], Marzia Capelletti[1,3], Ophélia Maertens[7,9], Eva M. Goetz[2,3], Anthony Letai[3], Levi A. Garraway[2,3,7,10], Matthew J. Lazzara[11], Neal Rosen[13,14], Nathanael S. Gray[4,6], Kwok-Kin Wong[1,3,5,7], and Pasi A. Jänne[1,3,5,7]

ABSTRACT

The clinical efficacy of epidermal growth factor receptor (EGFR) kinase inhibitors is limited by the development of drug resistance. The irreversible EGFR kinase inhibitor WZ4002 is effective against the most common mechanism of drug resistance mediated by the *EGFR* T790M mutation. Here, we show, in multiple complementary models, that resistance to WZ4002 develops through aberrant activation of extracellular signal-regulated kinase (ERK) signaling caused by either an amplification of mitogen-activated protein kinase 1 (*MAPK1*) or by downregulation of negative regulators of ERK signaling. Inhibition of MAP–ERK kinase (MEK) or ERK restores sensitivity to WZ4002 and prevents the emergence of drug resistance. We further identify *MAPK1* amplification in an erlotinib-resistant *EGFR*-mutant non–small cell lung carcinoma patient. In addition, the WZ4002-resistant *MAPK1*-amplified cells also show an increase both in EGFR internalization and a decrease in sensitivity to cytotoxic chemotherapy. Our findings provide insights into mechanisms of drug resistance to EGFR kinase inhibitors and highlight rational combination therapies that should be evaluated in clinical trials.

SIGNIFICANCE: Our study identifies activated ERK signaling as a mediator of resistance to irreversible pyrimidine EGFR inhibitors in *EGFR* T790M-bearing cancers. We further provide a therapeutic strategy to both treat and prevent the emergence of this resistance mechanism. *Cancer Discov; 2(10); 934–47. ©2012 AACR.*

Authors' Affiliations: [1]Lowe Center for Thoracic Oncology, [2]Center for Cancer Genome Discovery, [3]Department of Medical Oncology, [4]Department of Cancer Biology, and [5]Belfer Institute for Applied Cancer Science, Dana-Farber Cancer Institute; [6]Department of Biological Chemistry and Molecular Pharmacology, Harvard Medical School; Departments of [7]Medicine, [8]Pathology, and [9]Genetics Division, Brigham and Women's Hospital, Boston; [10]Broad Institute of Harvard and MIT, Cambridge, Massachusetts; [11]Department of Chemical and Biomolecular Engineering, University of Pennsylvania, Philadelphia, Pennsylvania; Departments of [12]Pediatrics, [13]Medicine, and [14]Molecular Pharmacology and Chemistry, Memorial Sloan-Kettering Cancer Center, New York, New York; and [15]Department of Molecular Pharmacology and Therapeutics, Oncology Institute, Loyola University Chicago, Stritch School of Medicine, Maywood, Illinois

Note: Supplementary data for this article are available at Cancer Discovery Online (http://www.cancerdiscovery.aacrjournals.org/).

Corresponding Author: Pasi A. Jänne, Lowe Center for Thoracic Oncology, Dana-Farber Cancer Institute, 450 Brookline Avenue, HIM 223, Boston, MA 02215. Phone: 617-632-6076; Fax: 617-582-7683; E-mail: pjanne@partners.org

doi: 10.1158/2159-8290.CD-12-0103

Published OnlineFirst September 7, 2012; DOI:10.1158/2159-8290.CD-12-0103

INTRODUCTION

Epidermal growth factor receptor (EGFR) kinase inhibitors gefitinib and erlotinib are effective clinical therapies for non–small cell lung cancer (NSCLC) patients harboring *EGFR*-mutant cancers. Several phase III clinical trials have showed improved clinical efficacy compared with systemic chemotherapy (1–3). However, despite these benefits, all patients ultimately develop acquired resistance to gefitinib and erlotinib (4). The most common mechanism of acquired resistance, detected in 50% to 60% of patients, is mediated by the secondary *EGFR* T790M mutation, and results in an increase in ATP affinity (5–8). In preclinical models, irreversible quinazoline-based EGFR inhibitors, including afatinib (BIBW2992) and dacomitinib (PF299804), effectively inhibit the growth of *EGFR* T790M-containing cell line models *in vitro* (9, 10). The covalent binding allows these inhibitors to achieve greater occupancy of the ATP site relative to gefitinib or erlotinib, thus providing the ability to inhibit EGFR T790M (8). However, in clinical studies, afatinib did not prolong survival compared with placebo in patients with NSCLC that had developed acquired resistance to gefitinib or erlotinib (11). Furthermore, in preclinical studies, resistance of *EGFR* T790M tumor cells to dacomitinib develops rapidly and is caused by amplification of the T790M-containing allele (12).

In an effort to overcome the therapeutic limitations of irreversible quinazoline EGFR inhibitors, we previously identified a novel class of irreversible pyrimidine-based EGFR kinase inhibitors (13). These agents, including WZ4002, are more potent than irreversible quinazoline EGFR inhibitors in *EGFR* T790M-bearing models, but are less potent inhibitors of wild-type (WT) EGFR (13). Coupled with the increased potency, the mutant selective property of this class of agents may provide the ability to achieve clinical concentrations sufficient to inhibit EGFR T790M.

In the current study, we modeled acquired resistance to WZ4002 in *EGFR* T790M-containing models *in vitro* and *in vivo*. We undertook these studies in an effort to identify potential strategies that can be used to enhance the efficacy of this class of EGFR inhibitors. Our studies identify a novel mechanism of resistance to EGFR inhibitors and inform the development of a novel combination therapeutic strategy that can be used to effectively treat *EGFR* T790M-containing cancers.

RESULTS

WZ4002-Resistant Cells Contain an Amplification in *MAPK1*

In our prior studies, we generated a gefitinib-resistant (GR) version of the *EGFR*-mutant PC9 (Del E746_A750) cell line (13). These cells contain the *EGFR* T790M resistance mutation and are sensitive to WZ4002 (13). When we exposed the PC9 GR cells to dacomitinib (PF299804), a clinical irreversible quinazoline EGFR inhibitor and generated resistant cells, they contained a focal amplification in *EGFR* preferentially involving the T790M allele (12). These PC9 dacomitinib-resistant (DR) cells are as sensitive to WZ4002 as the parental PC9 GR cells (Fig. 1A). To determine how cancers that harbor *EGFR* T790M develop resistance to WZ4002, we generated WZ4002-resistant (WZR) versions of the PC9 GR4 cells using previously established methods (12, 14). Several individual resistant clones were

Published OnlineFirst September 7, 2012; DOI:10.1158/2159-8290.CD-12-0103

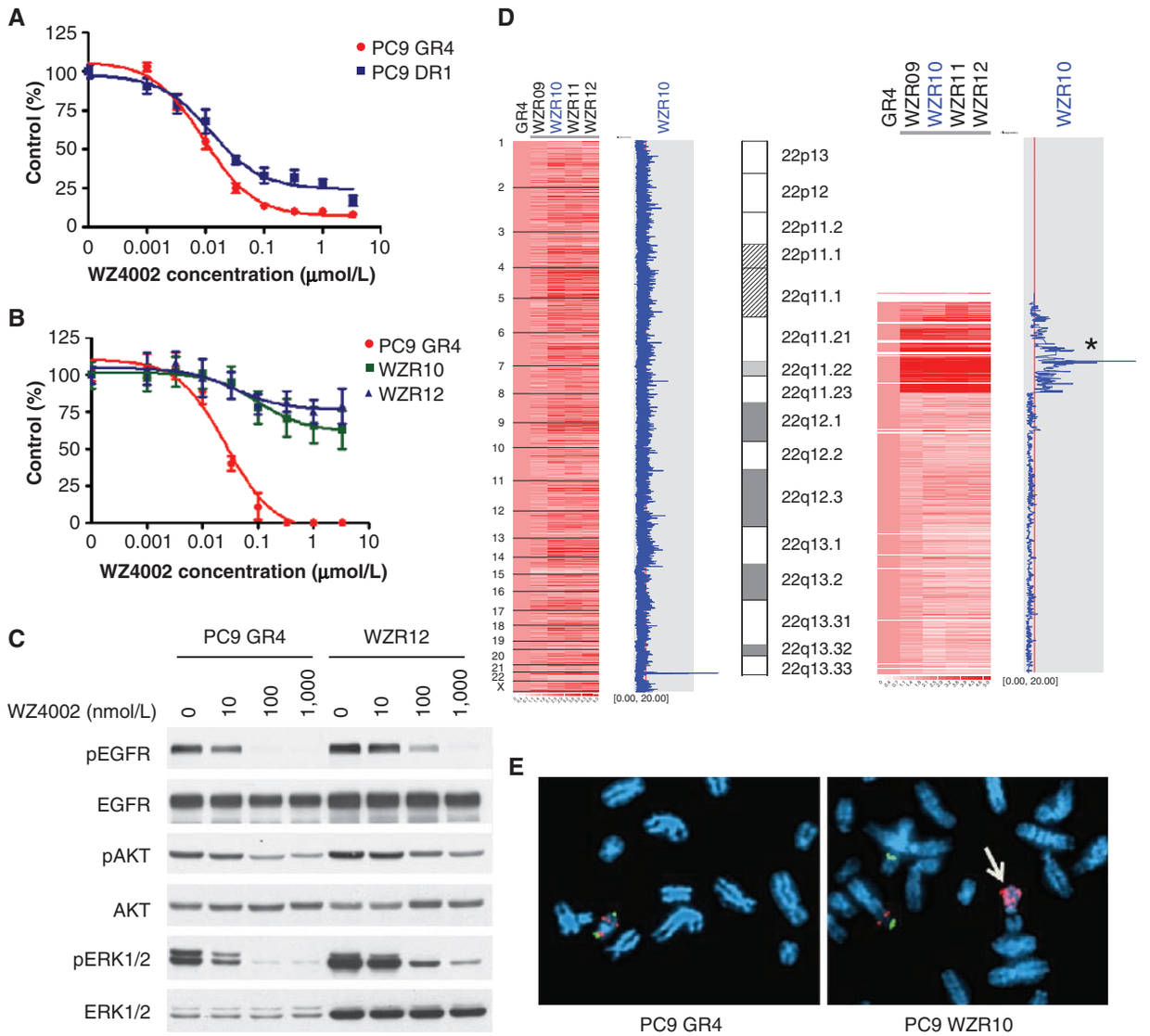

Figure 1. WZR *EGFR*-mutant Del E746_A750/T790M cells contain an amplification in *MAPK1*. **A,** PC9 GR4 (Del E746_A750/T790M) and DR1 (Del E746_A750/T790M amplification) cells were treated with WZ4002 at the indicated concentrations, and viable cells were measured after 72 hours of treatment and plotted relative to untreated controls. **B,** WZR10 and WZR12 cells are resistant to WZ4002. Cells were treated with WZ4002 as in **A. C,** PC9 GR4 and WZR12 cells were treated with WZ4002 at indicated concentrations for 6 hours. Cell extracts were immunoblotted to detect the indicated proteins. **D,** WZR cells contain an amplification in *MAPK1*. The PC9 WZR clones (right) were compared with the PC9 GR4 cells (first column). The blue curve on the right indicates degree of amplification of each SNP from 0 (left) to 8 (right). Left, genome-wide view; right, detailed view of chromosome 22. The genomic location of *MAPK1* is indicated by an asterisk. **E,** metaphase FISH of PC9 GR4 and WZR10 cells using *MAPK1* (red) and reference probe (green; RP11-768L22). Amplification of *MAPK1* is observed in WZR10 cells (arrow).

identified and confirmed to be drug resistant (Fig. 1B). The resistant cells still harbored the *EGFR* Del E746_A750/T790M double mutation but contained no additional *EGFR* mutations (data not shown) and were also cross resistant to dacomitnib and afatinib (data not shown). WZ4002 still inhibited EGFR phosphorylation in the resistant cells, although slightly less potently in the GR4 cells, but more noticeably, this inhibition was decoupled from inhibition of downstream signaling most notably extracellular signal-regulated kinase 2 (ERK2) phosphorylation (Fig. 1C). The WZR12 cells contain higher levels of both total and phosphorylated ERK2 than the PC9 GR cells (Fig. 1C). To determine whether there was a genomic basis for the increase in ERK2 protein, we conducted a genome-wide copy number analysis of the WZR cells and compared them to the parental PC9 GR4 cells (Fig. 1D). The WZR cells contain an amplification in chromosome 22 that is not present in the parental drug-sensitive cell line. This region contains the gene mitogen-activated protein kinase 1 (*MAPK1*), which encodes ERK2 (Fig. 1D). We confirmed the *MAPK1* amplification using both FISH (Fig. 1E.) and quantitative real-time PCR [qRT-PCR (Supplementary Fig. S1)]. The amplification also led to increased *MAPK1* gene expression (Supplementary Fig. S2A).

Published OnlineFirst September 7, 2012; DOI:10.1158/2159-8290.CD-12-0103

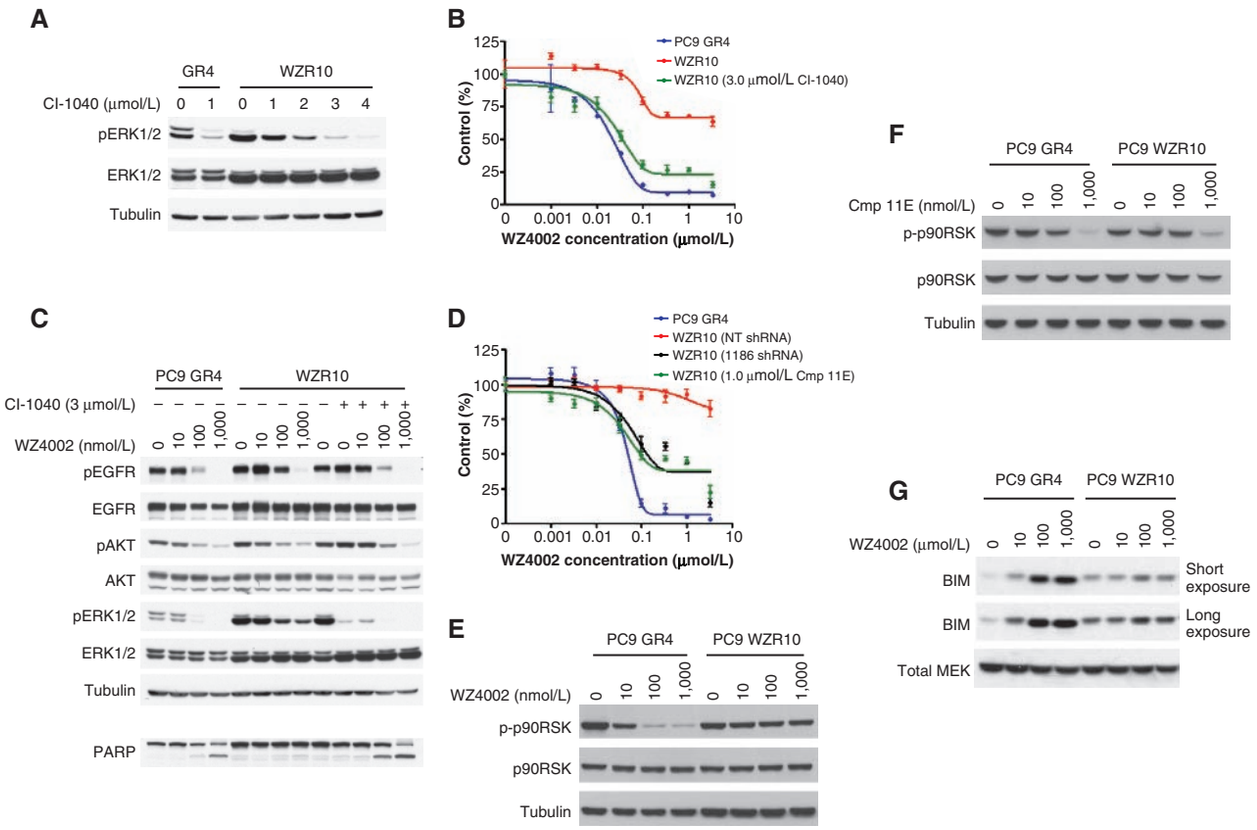

Figure 2. Inhibition of ERK1/2 signaling restores sensitivity to WZ4002 in PC9 WZR cells. **A,** PC9 GR4 or WZR10 cells were treated with the indicated concentrations of CI-104 for 6 hours. Cell extracts were immunoblotted to detect the indicated proteins. **B,** PC9 GR4 or WZR10 cells were treated with WZ4002 alone at the indicated concentrations or in combination with CI-1040 (3 μmol/L). Viable cells were measured after 72 hours of treatment and plotted relative to untreated controls. **C,** PC9 GR4 or WZR10 cells were treated with WZ4002 alone at indicated concentrations or with CI-1040 (3 μmol/L) for 6 or 48 hours (PARP lane only). Cell extracts were immunoblotted to detect the indicated proteins. **D,** cells were treated with WZ4002 at the indicated concentrations or in combination with Compound (Cmp) 11E (WZR10 only). Viable cells were measured after 72 hours of treatment and plotted relative to untreated controls. **E,** WZ4002 (6 hours) inhibits p90RSK phosphorylation in PC9 GR4 but not WZR10 cells. **F,** Cmp 11E (6 hours) inhibits p90RSK phosphorylation in both PC9 GR4 and WZR10 cells. **G,** WZ4002 treatment (6 hours) leads to BIM upregulation in PC9 GR4 but not WZR10 cells.

Inhibition of MAPK Signaling Restores Sensitivity to WZ4002

We next evaluated whether inhibition of MAPK signaling would restore sensitivity to WZ4002 in the PC9 WZR cells. We first determined the concentration of the MAP–ERK kinase (MEK) inhibitor CI-1040 necessary to downregulate ERK1/2 phosphorylation to similar levels as in the parental cell lines (Fig. 2A). When used in combination with WZ4002, the MEK inhibitors CI-1040 (Fig. 2B) or GSK-1120212 (Supplementary Fig. S3) completely restored the sensitivity to WZ4002 in the WZR cells similar to that of the parental PC9 GR4 cells. Similarly, the combination led to complete inhibition of ERK1/2 phosphorylation and restored WZ4002-mediated apoptosis analogous to that observed in the parental PC9 GR cells (Figs. 2C and Supplementary Fig. S4). WZ4002 sensitivity was also restored following downregulation of *MAPK1* using a *MAPK1*-specific short hairpin (sh)-RNA (Supplementary Fig. S5 and Fig. 2D), or when WZ4002 was combined with an ERK1/2 kinase inhibitor (compound 11e; Fig. 2D; ref. 15). Inhibition of ERK1/2 using compound 11e also restored WZ4002-mediated apoptosis in the PC9 WZR cells (Supplementary Fig. S4). As a pharmacodynamic measure of compound 11e, we evaluated p90RSK phosphorylation, a known ERK substrate (16). In the PC9 GR cells, but not in the WZR cells, WZ4002 treatment inhibited p90RSK phosphorylation (Fig. 2E). However, in both GR4 and WZR10 cells, compound 11e was able to inhibit p90RSK phosphorylation (Fig. 2F). The addition of a dual phosphoinositide 3-kinase (PI3K) and mTOR inhibitor, PI103, or the AKT inhibitor MK-2206, did not restore sensitivity to WZ4002, nor did it result in WZ4002-mediated apoptosis (Supplementary Figs. S6A–C; refs. 17, 18).

To further show the role of activated MAPK signaling in mediating WZ4002 resistance, we introduced an activated *MEK1* (*MEK1* K57N) allele into the PC9 GR or H1975 cells (Supplementary Fig. S7; ref. 19). This led to WZ4002 resistance, and in the resistant cells WZ4002 treatment no longer resulted in complete inhibition of ERK1/2 phosphorylation or induction of apoptosis (Supplementary Fig. S7A and B). In addition, *MEK1* K57N was sufficient to cause resistance to both WZ4002 (data not shown) and to gefitinib (Supplementary Fig. S7C) when introduced into the drug-sensitive

Published OnlineFirst September 7, 2012; DOI:10.1158/2159-8290.CD-12-0103

PC9 (Del E746_A750) cells. Collectively, our findings suggest that activation of MAPK signaling causes WZ4002 resistance.

We further evaluated how *MAPK1* amplification may prevent WZ4002-mediated apoptosis. Prior studies have shown that upregulation of the proapoptotic protein BIM was necessary for EGFR-mediated apoptosis in *EGFR*-mutant cancers (20–22). BIM upregulation is mediated by ERK signaling (20–22). In the PC9 GR4 cells, WZ4002 treatment led to a dose-dependent upregulation of BIM (Fig. 2G). In contrast, in the PC9 WZR cells, BIM upregulation was blunted consistent with the inability for WZ4002 to fully downregulate ERK1/2 phosphorylation in these cells (Figs. 1C and 2G).

H1975 WZ4002-Resistant Cells Retain ERK1/2 Signaling But Do Not Contain an Amplification of *MAPK1*

We also generated resistant versions of the WZ4002-sensitive H1975 (EGFR L858R/T790M) cell line (Fig. 3A). Similar to the PC9 WZR cells, WZ4002 was still able to inhibit EGFR phosphorylation in the H1975 WZR cells but ERK1/2 phosphorylation was not completely inhibited (Fig. 3B). The H1975 WZR cells did not contain additional *EGFR* mutations, did not contain an amplification or overexpression of *MAPK1* (Supplementary Fig. S2B), and did not harbor other regions of genomic gain when compared with the parental cells (data not shown). The MEK inhibitor CI-1040, but not the PI3K/mTOR inhibitor PI-103 (Supplementary Fig. S6D), restored sensitivity to WZ4002 in the H1975 WZR cells (Fig. 3C). Furthermore, in the presence of CI-1040, WZ4002 treatment led to complete inhibition of ERK1/2 phosphorylation as in the parental cells (Fig. 3D). To understand the mechanism behind sustained ERK1/2 activation in the H1975 WZR cells, we compared genome-wide mRNA expression between H1975 WZR6 and H1975 cells (Fig. 3E). One of the most downregulated genes in H1975 WZR cells compared with H1975 cells was *DUSP6*, a dual specificity phosphatase that negatively regulates ERK1/2 phosphorylation (23). We confirmed these findings using qRT-PCR and also observed downregulation of *DUSP5*, *SPRY4,* and *SPRED2*, all of which negatively regulate components of MAPK signaling (refs. 24–26; Fig. 3F). We did not observe downregulation of these genes in the PC9 WZR cells (Supplementary Fig. S8A). Downregulation of *DUSP6* using an siRNA was sufficient to cause resistance to WZ4002 in PC9 GR4 cells (Fig. 3G) and to both gefitinib and WZ4002 in PC9 cells (Supplementary Fig. S8B). Our findings suggest that downregulation of negative regulators of MAPK signaling and subsequent activation of ERK1/2 signaling is an alternative mechanism that mediates WZ4002 resistance. Furthermore, activation of ERK1/2 signaling through introduction of *MEK1* K57N into H1975 cells was also sufficient to cause WZ4002 resistance (Supplementary Fig. S7D).

ERK1/2 Signaling Mediates Resistance to WZ4002 in a Murine Model of *EGFR* T790M Lung Cancer

We previously showed that WZ4002 is effective *in vivo* using murine models of *EGFR* T790M (L858R/T790M and Del E746_A750/T790M) NSCLC over a 2-week treatment course (13). With prolonged treatment, although we observed increased survival compared with erlotinib in both *EGFR* T790M-bearing models (Fig. 4A), we also observed the development of acquired resistance (Figs. 4B and C and Supplementary Figs. S9A and B). At the time of resistance, we examined the tumors from the treated mice and noted that although EGFR phosphorylation was still inhibited by WZ4002, we were able detect the emergence of robust expression of ERK1/2 phosphorylation (Figs. 4D and E and Supplementary Fig. S10). In contrast, short-term (24-hour) treatment with WZ4002 effectively inhibits both EGFR and ERK1/2 phosphorylation in the mouse tumors (Fig. 4E). We did not detect evidence of *Mapk1* amplification by FISH in the resistant tumors (Supplementary Fig. S11A), evidence of *Kras* mutations (data not shown), or loss of NF1, a negative regulator of MAPK signaling, at either the protein (Supplementary Fig. S11B) or RNA (Supplementary Fig. S11C) level (27). However, some of the resistant tumors had evidence of decreased *Dusp6* expression compared with their drug-sensitive counterparts (Supplementary Fig. S12). Given the persistent ERK1/2 signaling in the WZR tumors, we investigated whether a clinical MEK inhibitor, GSK-1120212, could restore the sensitivity to WZ4002 *in vivo*. Following the development of acquired resistance to WZ4002 (after 19, 20, and 28 weeks of therapy), we switched treatment to the combination of WZ4002 and GSK-1120212 (Fig. 4F). In 3/3 mice, GSK-1120212-restored sensitivity to WZ4002 (Figs. 4G and H).

An alternative strategy to treating drug resistance is to delay or prevent it from occurring. To determine whether this strategy may be applicable to the current model, we evaluated this using an *in vitro* model. We exposed the WZ4002-sensitive PC9 GR (Fig. 4I) or H1975 (Fig. 4J) cells to either WZ4002 alone, CI-1040 alone, or the combination of both agents for 3 months and quantified resistant clones. CI-1040 was ineffective in both models whereas WZ4002 alone led to a decreased number of resistant clones only in the PC9 GR4 cells (Fig. 4I). However, the combination of WZ4002/CI-1040 was significantly more effective at preventing the emergence of drug-resistant clones in both models (Figs. 4I and J).

MAPK1 Amplification Is Present in an Erlotinib-Resistant NSCLC Patient

Our preclinical studies suggest that reactivation of ERK1/2 signaling not only can mediate resistance to WZ4002 but also to geftinib in drug-sensitive *EGFR*-mutant NSCLC cell lines (Supplementary Fig. S7C). We thus evaluated tumor specimens from erlotinib-treated NSCLC patients that had developed drug resistance (Supplementary Table S1) for the presence of *MAPK1* amplification. In 1 of 21 patients (4.8%) examined, we identified a *MAPK1* amplification that was not present in the pretreatment drug-sensitive tumor specimen (Fig. 5). The resistant tumor also lacked the more common drug-resistance mechanisms *EGFR* T790M or *MET* amplification (data not shown).

MAPK1 Amplification Leads to an Increase in EGFR Internalization

We initially noticed that despite the absence of *EGFR* secondary mutations in the PC9 WZR cells, 10 times greater concentrations of WZ4002 were required to inhibit EGFR phosphorylation (Fig. 1C and 6A). This observation could be because of the presence of mutant or WT phosphorylated EGFR [the PC9 GR and WZR cells are both heterozygous for

Published OnlineFirst September 7, 2012; DOI:10.1158/2159-8290.CD-12-0103

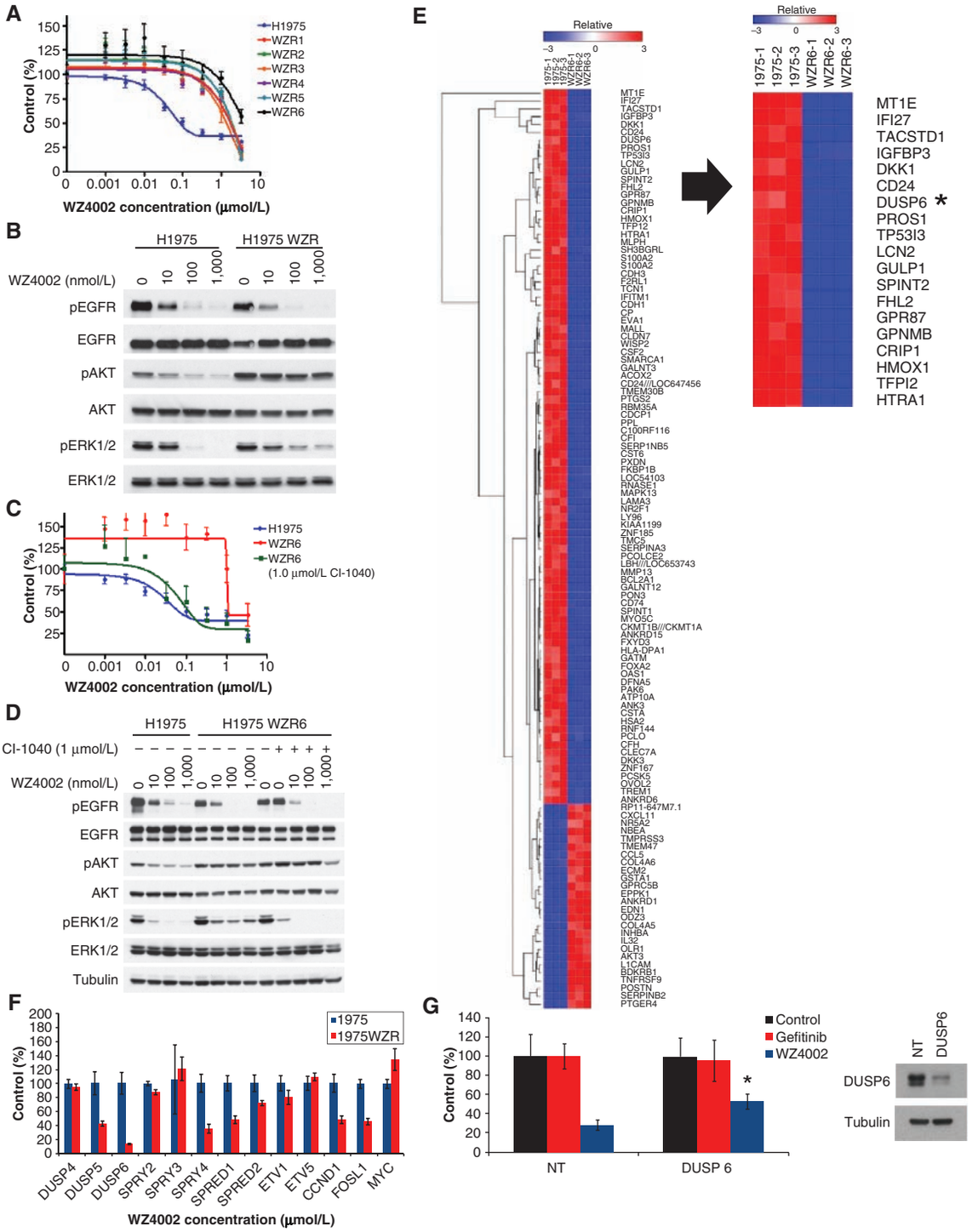

Figure 3. WZR H1975 cells exhibit persistent ERK activation and MEK inhibition restores WZ4002 sensitivity. **A,** WZR H1975 clones. Cells were treated with WZ4002 at the indicated concentrations, and viable cells were measured after 72 hours of treatment and plotted relative to untreated controls. **B,** WZ4002 treatment does not fully inhibit ERK1/2 phosphorylation in WZR6 cells. H1975 and H1975 WZR6 cells were treated with increasing concentrations of WZ4002. Cell extracts were immunoblotted to detect the indicated proteins. **C,** CI-1040 (1 μmol/L) restores sensitivity to WZ4002 in the WZR6 cells. **D,** CI-1040 (1 μmol/L) restores the ability of WZ4002 to fully inhibit ERK1/2 phosphorylation in the WZR6 cells. **E,** comparison of expression profiles of H1975 and WZR6 cells (left). Hierarchical clustering of the differentially expressed genes [$P < 0.0025$, fold change (FC) > 3.9] was conducted using GENE-E. *DUSP6* (asterisk) ranks among the top differentially expressed genes (right). **F,** qRT-PCR of genes in MEK/ERK transcriptional output in H1975 and H1975 WZR cells. The data are normalized to the H1975 cells. Error bars denote standard deviation. **G,** PC9 GR4 cells were treated with gefitinib (1 μmol/L) or WZ4002 (100 nmol/L) following transfection with control (NT) or *DUSP6* siRNA and viable cells were measured after 48 hours of treatment and plotted (mean ± SD) relative to untreated controls. *, $P < 0.05$ *DUSP6* versus NT.

Published OnlineFirst September 7, 2012; DOI:10.1158/2159-8290.CD-12-0103

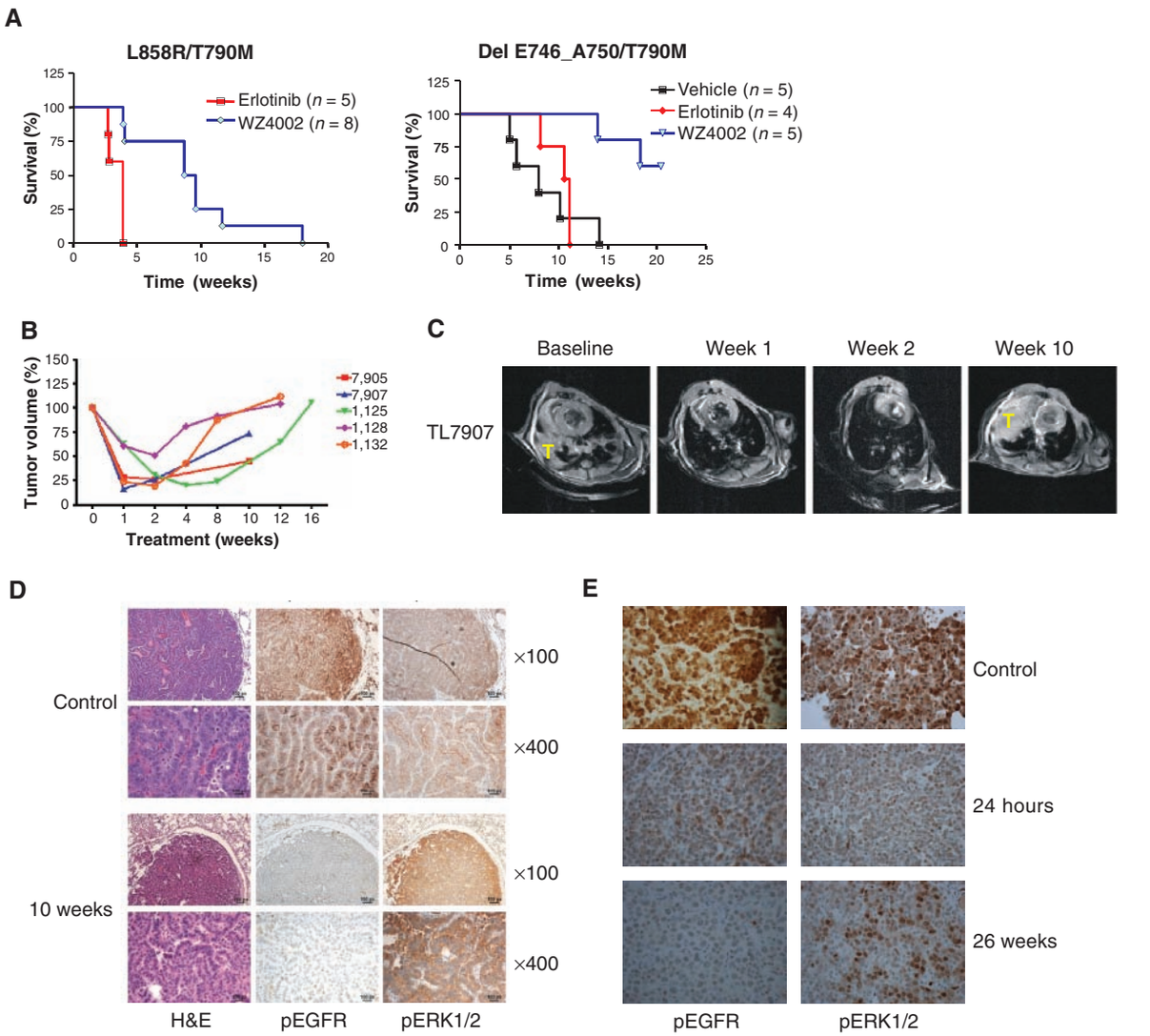

Figure 4. Development of *in vivo* resistance to WZ4002 in genetically engineered mouse models of *EGFR* T790M. **A,** Kaplan–Meier survival curves of L858R/T790M or Del E746_A750/T790M mice treated with erlotinib, vehicle, or WZ4002. Treatment with WZ4002 significantly prolongs survival compared with erlotinib [$P = 0.0015$ (L858R/T790M) and $P = 0.0064$ (Del E746_A750/T790M); both log-rank test]. **B,** change in tumor volume over time in *EGFR* L858R/T790M mice ($n = 5$) treated with WZ4002. Each curve represents an individual mouse. **C,** MRI images from mouse 7907 from **B.** T, tumor. **D,** immunohistochemical analyses using indicated antibodies of tumors from *EGFR* L858R/T790M untreated and WZ4002 treated (10 weeks) mice. EGFR phosphorylation but not ERK1/2 phosphorylation is inhibited. H&E, hematoxylin and eosin. **E,** immunohistochemical analyses using indicated antibodies of tumors from EGFR Del E746_A750/T790M untreated and WZ4002 treated (24 hours and 26 weeks) mice. WZ4002 treatment inhibits both EGFR and ERK1/2 phosphorylation at 24 hours but ERK1/2 phosphorylation returns following 26 weeks of therapy. (*continued*)

Del E746_A750 (data not shown)]. We immunoprecipitated the mutant EGFR from the PC9 GR4 and WZR cells using a mutant-specific (EGFR Del E746_A750M) EGFR antibody (Fig. 6A) following WZ4002 treatment. Compared with the PC9 GR4 cells, greater concentrations of WZ4002 were required to inhibit Del E746_A750/T790M consistent with the observations in whole cell lysates (Fig. 6A). One potential explanation for these differences is an alteration in EGFR internalization. An alteration in EGFR internalization could lead to changes in cellular localization of EGFR that may impact drug access and hence the need for an increased drug concentration required to inhibit EGFR phosphorylation. We evaluated EGFR internalization using ^{125}I labeled EGF. In both the WZR10 and 12 cells, we observed a significantly larger internalization rate constant (k_e) than in the GR4 cells (Fig. 6B). There was no difference between the PC9 GR4 and the PC9 cells (Fig. 6B). Inhibition of MEK using CI-1040 did not alter k_e in GR4 cells, but significantly, although not completely, reduced both EGFR phosphorylation and k_e in the WZR cells to levels similar to that observed in the parental PC9 GR4 cells (Figs. 6C and D). Prior studies have implicated Thr-669 of EGFR as an ERK phosphorylation site and associated with EGFR turnover possibly through internalization (28–30). This site is highly phosphorylated in the PC9 WZR

Published OnlineFirst September 7, 2012; DOI:10.1158/2159-8290.CD-12-0103

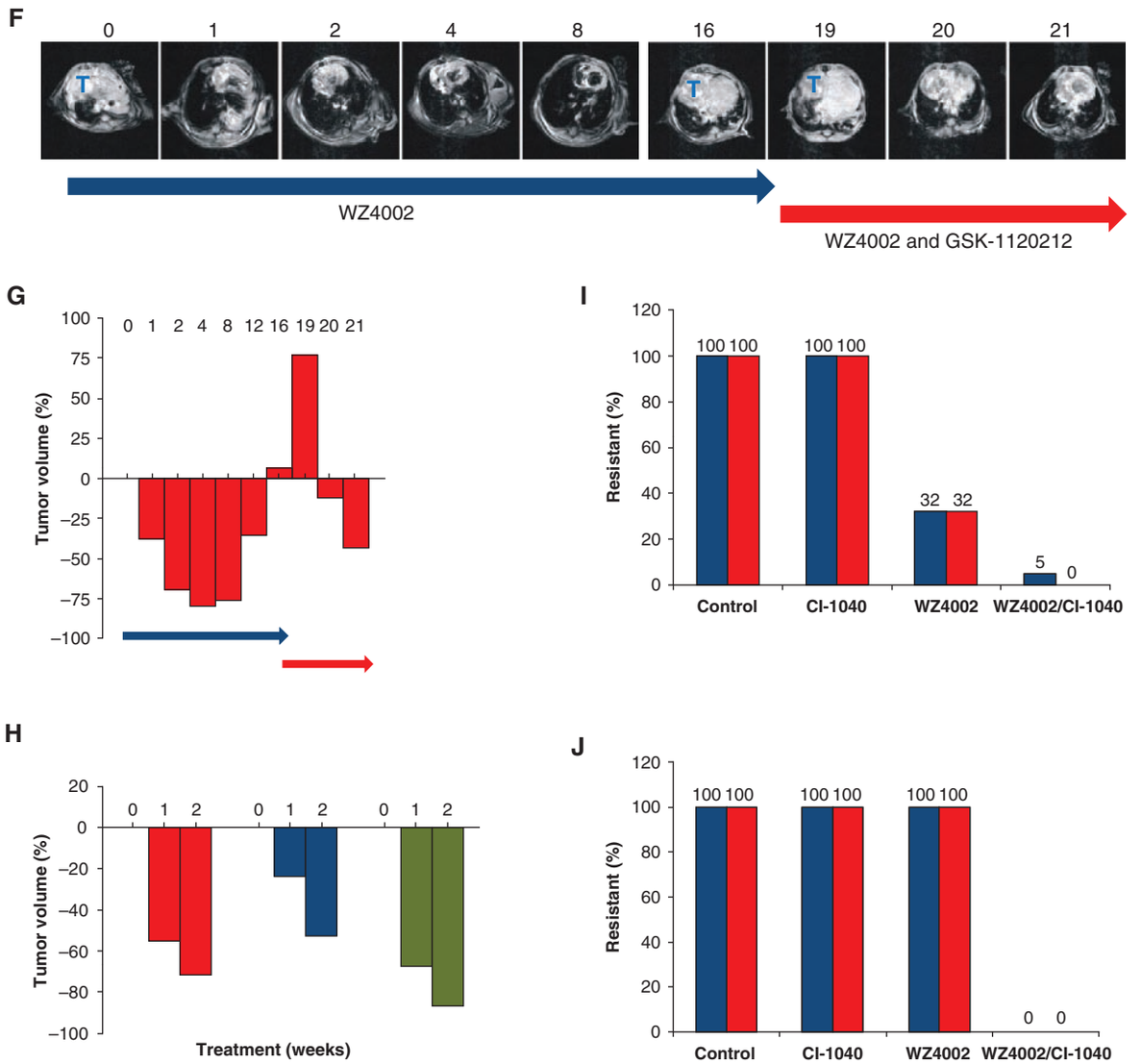

Figure 4. ***(Continued)*** **F,** serial MRI images of an *EGFR* L858R/T790M mouse treated with WZ4002 alone or with the combination of WZ4002 and GSK-1120212. T, tumor. **G,** tumor volume measurements from mouse in **F.** Blue arrow, treatment with WZ4002; red arrow; treatment with both WZ4002 and GSK-1120212. Numbers indicate weeks of treatment. **H,** waterfall plot of tumor volume from 3 L858R/T790M mice following treatment with WZ4002 and GSK-1120212. **I,** Long-term treatment of PC9 GR4 cells with CI-1040 alone, WZ4002 alone, or the combination of both drugs. The percentages of resistant colonies relative to control are plotted from 2 independent experiments. **J,** long-term treatment of H1975 cells with CI-1040 alone, WZ4002 alone, or the combination of both drugs. The percentages of resistant colonies relative to control are plotted from 2 independent experiments.

cells compared with the parental PC9 GR4 cells (Fig. 6E) and is inhibited by CI-1040 treatment alone without affecting the EGFR autophosphorylation site on Tyr 1068 (Fig. 6E). We did not observe any changes in k_e in the H1975 WZR cells (data not shown).

Successive Tyrosine Kinase Inhibitor Resistance Also Leads to Chemotherapy Resistance

Following the development of clinical resistance to EGFR kinase inhibitors, NSCLC patients are often treated with systemic chemotherapy. Our successive cell line models (PC9, gefitinib and WZ4002 sensitive; PC9 GR, gefitinib resistant but WZ4002 sensitive; and PC9 WZR, gefitinib and WZR) provide a system in which to evaluate whether kinase inhibitor resistance impacts chemotherapy sensitivity. We treated the cells with staurosporine, paclitaxel, and etoposide. As can be seen in Fig. 7A, these agents induce the greatest degree of cell death in the parental PC9 cells and the least in the PC9 WZR cells. All 3 of these agents, as well as EGFR inhibitors, are known to kill via the mitochondrial pathway of apoptosis, suggesting that cells may select for resistance to apoptosis more generally when they select for resistance to tyrosine kinase inhibition (21). MEK inhibition in PC9 WZR cells did not reverse resistance to chemotherapy (data not shown). It has recently been shown that

Published OnlineFirst September 7, 2012; DOI:10.1158/2159-8290.CD-12-0103

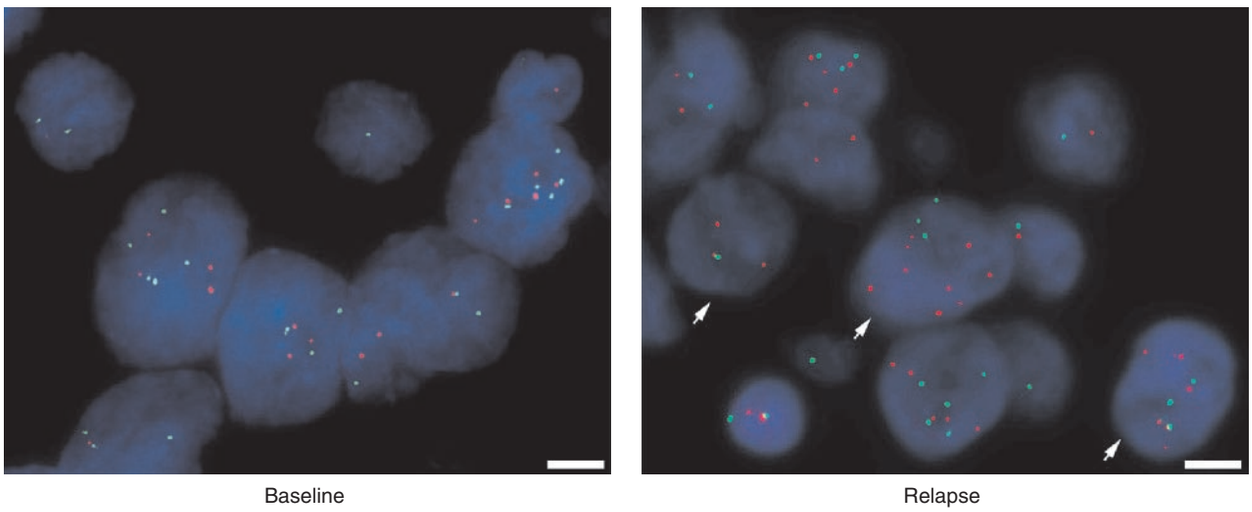

Figure 5. *MAPK1* amplification is present in erlotinib-resistant *EGFR*-mutant NSCLC. FISH analysis of a baseline (left) and a post–erlotinib-treated tumor (right). There is evidence of *MAPK1* amplification (arrows) in the relapsed tumor. *MAPK1* (red), 22q13.33 reference probe (green; RP11-768L22). Scale bar, 5 μm.

one can measure pretreatment proximity of the mitochondria to the apoptotic threshold, known as mitochondrial priming, using BH3 profiling (31). Proximity to the threshold, indicated by increased mitochondrial depolarization in response to BH3 peptides, was shown to correlate to chemosensitivity across a broad range of cancers (31). We found that the successive generations of kinase inhibitor–resistant PC9 cells were indeed less primed (Fig. 7B). This result suggests that a more broad resistance to apoptotic signaling may be selected for when cells select for tyrosine kinase inhibitor (TKI) resistance.

DISCUSSION

Despite the dramatic clinical efficacy of EGFR kinase inhibitors in *EGFR*-mutant NSCLC, single-agent EGFR inhibitors will not cure advanced NSCLC. Studies of drug resistance mechanisms provide insights into how cancers develop resistance and the findings from these studies can be used to design rational combination therapeutic strategies (14). *EGFR* T790M is the most common mechanism of acquired drug resistance to erlotinib and gefitinib and, to date, has also been the most difficult to treat clinically (5–7, 11). This is mirrored by our prior preclinical studies using a clinical irreversible quinazoline EGFR inhibitor (PF299804 or dacomitinib; ref. 12). Although the PC9 GR cells are transiently sensitive to PF299804, resistant cells harboring *EGFR* T790M amplification rapidly emerge (12). These *EGFR* T790M-amplified cells retain sensitivity to the mutant-selective EGFR inhibitor WZ4002 (Fig. 1A) and remarkably, *EGFR* T790M amplification never emerges as a resistance mechanism when PC9 GR4 cells are exposed to WZ4002. These findings not only highlight the potential clinical efficacy of a more potent EGFR inhibitor but also the rapid ability of cancer cells to adapt to such an inhibitor as we are still able to select WZR clones from the PC9 GR cells.

Previous studies have implicated maintenance of PI3K signaling as critical in mediating resistance to EGFR kinase inhibitors (32, 33). Resistance mechanisms to EGFR TKIs include *MET* amplification, hepatocyte growth factor (HGF) production, and *PIK3CA* mutations, all of which block gefitinib- or erlotinib-mediated inhibition of AKT phosphorylation (14, 32, 34). Inhibition of PI3K signaling using PI-103 alone or in combination with gefitinib has been shown to overcome HGF-mediated resistance to gefitinib both *in vitro* and *in vivo* (35). Our current findings suggest that resistance to EGFR inhibitors can also arise through persistent or reactivation of ERK1/2 signaling. This can occur through at least 2 independent mechanisms: genomic amplification of *MAPK1* and downregulation of negative regulators of ERK1/2 signaling (Figs. 1D and 3F). These drug-resistant cells are not ERK dependent as MEK or ERK inhibition alone is not sufficient to restore apoptosis but rather requires concomitant EGFR inhibition (Figs. 2B and D). In contrast to HGF-mediated resistance, PI3K or AKT inhibition alone or in combination with WZ4002 is not sufficient to reverse drug resistance as PI3K inhibition does not result in ERK1/2 inhibition (Supplementary Figs. S6; ref. 35). Thus, the therapeutic strategy for overcoming EGFR inhibitor resistance needs to be tailored based on the specific signaling pathways activated by each of the resistance mechanisms.

We further show that our findings have clinical relevance as *MAPK1* amplification can also emerge in erlotinib-resistant *EGFR*-mutant NSCLC patients (Fig. 5). The frequency at which this occurs is low (Supplementary Table S1) but not unexpected, given the high prevalence of *EGFR* T790M as an erlotinib resistance mechanism (7). These observations may be because of the preexistence of *EGFR* T790M in some treatment-naïve cancers coupled with the current lack of effective clinical therapies against *EGFR* T790M (11, 36). This hypothesis is supported by preclinical studies of the PC9 cells in which multiple studies show the emergence of *EGFR* T790M following exposure to first- or second-generation EGFR TKIs

Published OnlineFirst September 7, 2012; DOI:10.1158/2159-8290.CD-12-0103

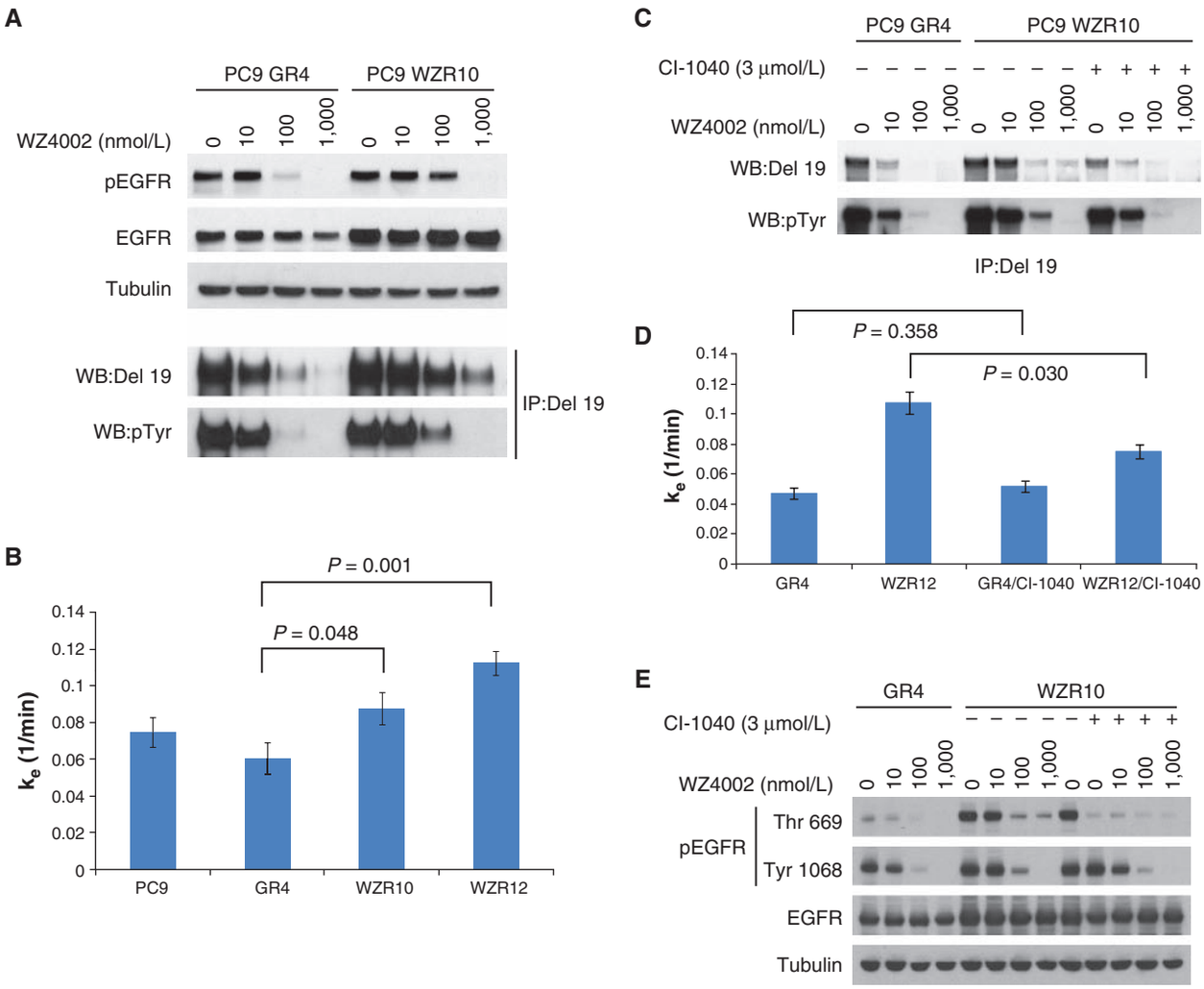

Figure 6. *MAPK1* amplification alters EGFR internalization. **A,** PC9 GR4 or WZR10 cells are treated with increasing concentrations of WZ4002 for 6 hours. Cell extracts from whole lysates (top) or following immunoprecipitation with an EGFR Del E746_A750 antibody (bottom) were immunoblotted to detect the indicated proteins. **B,** internalization rate constants (k_e) for ^{125}I-labeled EGF in different cell lines. The k_e is significantly greater for the WZR cells compared with the PC9 GR4 cells. **C,** PC9 GR4 and WZR10 cells treated with WZ4002 alone or in combination with CI-1040 for 6 hours. Cell extracts following immunoprecipitation with an EGFR Del E746_A750 antibody were immunoblotted to detect the indicated proteins. **D,** internalization rate constants (k_e) for ^{125}I-labeled EGF in following treatment with CI-1040 (3 mmol/L) for 24 hours. There is a significant reduction in k_e in the WZR10 cells with CI-1040 treatment. **E,** EGFR phosphorylation at Thr-669 is markedly increased in WZR10 compared with GR4 cells. CI-1040 alone inhibits phosphorylation at Thr-669 but not Tyr-1068.

(37–39). In contrast, WZR PC9 cells do not harbor EGFR T790M (13). As EGFR T790M-directed inhibitors, including CO-1686 (NCT01526928), enter clinical development, *MAPK1* amplification may begin to emerge as a more common resistance mechanism, and should be evaluated, along with other mechanisms leading to reactivation of ERK signaling, in tumor specimens when clinical drug resistance develops.

Our study also identifies 2 unique aspects of drug resistance mediated by *MAPK1* amplification and serves to highlight the complexity of drug-resistance mechanisms. In addition to its effects on signaling, *MAPK1* amplification correlates with changes in EGFR internalization (Fig. 6B). This leads to a 10-fold increase in the concentration of WZ4002 required to fully inhibit EGFR phosphorylation (Fig. 6A). Although this difference may at first glance seem subtle, in cancer patients receiving therapy with a kinase inhibitor, this change in drug concentration required for target inhibition could be the difference between a clinically sensitive and resistant tumor. Previous studies have shown a reduced rate of ligand-mediated EGFR internalization in drug-sensitive *EGFR*-mutant NSCLC cell lines (40). The decreased rate of EGFR endocytosis was found to be associated with an impaired ability of EGFR to fully use SHP2 for complete activation of ERK signaling (40). In contrast, enhanced ERK signaling, as observed in the PC9 WZR cells, plays a causal role in increased EGFR endocytosis. This observation may be because of the ability of ERK to phosphorylate EGFR at Thr-669, as observed in the WZR cells (Fig. 6E), leading to

Published OnlineFirst September 7, 2012; DOI:10.1158/2159-8290.CD-12-0103

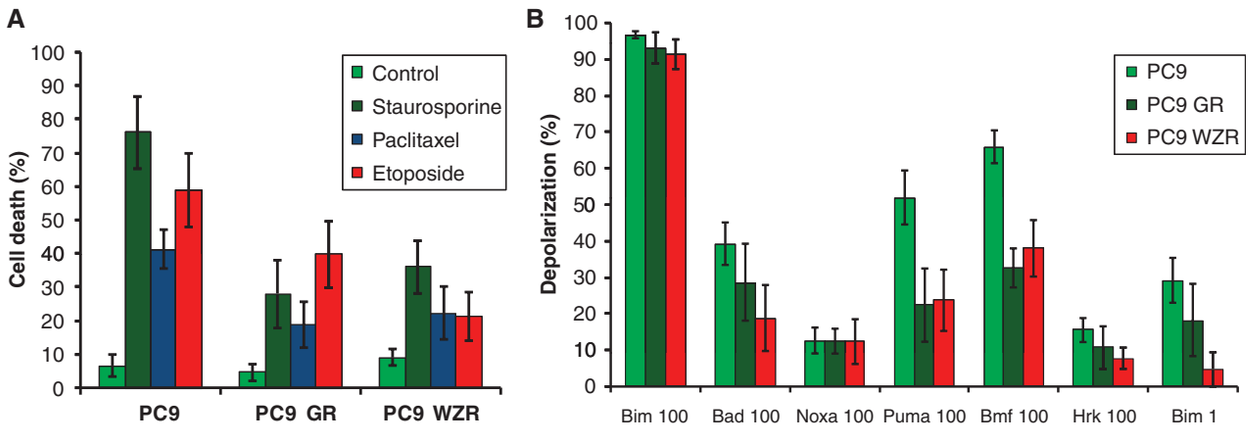

Figure 7. EGFR TKI-resistant PC9 cells are also more resistant to cytotoxic chemotherapy. **A,** cell viability experiments following 24 hours' exposure to staurosporine (1 μmol/L), paclitaxel (1 μmol/L), or etoposide (100 μmol/L). Dimethyl sulfoxide (DMSO) was used as a control. The mean values and standard deviation from 3 independent experiments are shown. **B,** mitochondrial depolarization response to BH3 peptides for PC9, PC9 GR4, and WZR10 cells. The mean values and standard deviation from 3 independent experiments are shown.

altered EGFR trafficking (28–30). Although clinically relevant, it will remain a challenge to study changes in receptor internalization from clinical diagnostic specimens unless they are because of a genomic alteration, as in the current study. Our findings also reveal that sequential resistance to kinase inhibitors (gefitinib and WZ4002) renders *EGFR*-mutant NSCLC cells less susceptible to chemotherapeutic agents (Fig. 7B). These observations are potentially clinically significant as EGFR kinase inhibitors are currently being used as initial therapy for *EGFR*-mutant NSCLC and may ultimately impact the sensitivity to a broad range of subsequent therapies (2, 3). These findings also serve to highlight that drug resistance may not simply be an alteration in one signaling pathway but rather a more complex process that more broadly impacts apoptotic signaling.

Findings from our study show that the combination of WZ4002 and an allosteric MEK inhibitor may be an effective strategy not only to treat drug-resistant cancers (Figs. 2B, 3C, and 4G and H) but also to prevent the emergence of drug-resistant clones (Fig. 4I and J). Coupled with our prior studies showing that WZ4002 alone can prevent the emergence of *EGFR* T790M in model systems, the combination of WZ4002 and a MEK inhibitor may be a particularly effective therapeutic strategy for *EGFR*-mutant NSCLC and should be tested in a clinical trial (13).

METHODS

Cell Culture and Reagents

The *EGFR*-mutant NSCLC cell lines PC9 (Del E746_A750), PC9 GR4 (Del E746_A750/T790M), and H1975 (L858R/T790M) have been previously characterized (12, 13, 41). The PC9 and H1975 cells were confirmed by fingerprinting using the Power Plex 1.2 system (Promega) most recently in March 2012. Gefitinib, CI-1040, and MK-2206 were obtained from Selleck Chemicals. WZ4002 was synthesized using previously published methods (13). GSK-1120212 was synthesized at Haoyuan Chemexpress according to published methods (42). Compound 11e was synthesized as previously described (15). Stock solutions of all drugs were prepared in dimethyl sulfoxide (DMSO) and stored at −20°C. *DUSP6* and control (nontargeting; NT) siRNA reagents were obtained from Dharmacon and used according to the manufacturer's recommended conditions.

Cell Proliferation and Growth Assays

Growth and inhibition of growth was assessed by MTS assay according to previously established methods (32, 43, 44). All experimental points were set up in 6 to 12 wells and all experiments were repeated at least 3 times. The data were graphically displayed using GraphPad Prism version 5.0 for Windows (GraphPad Software Inc.). Long-term drug treatment studies were conducted in 96-well format using 100 wells for each condition and conducted in triplicate. Resistant wells were assayed following 3 months of treatment and are plotted relative to untreated cells.

Antibodies and Western Blotting

Cells grown under the previously specified conditions were lysed in NP-40 buffer. Western blot analyses were conducted after separation by SDS-PAGE electrophoresis and transfer to polyvinylidene difluoride-P immobilon membranes (Millipore). Immunoblotting was conducted according to the antibody manufacturers' recommendations. Anti–phospho-AKT (Ser-473), anti–total-AKT, EGFR Del E746_A750 specific, phospho (Thr-669) EGFR, pRSK, total-RSK, DUSP6, and BIM antibodies were obtained from Cell Signaling Technology. The phospho-EGFR (pY1068), total-ERK1/2, and phospho-ERK1/2 (pT185/pY187) antibodies were purchased from Biosource International Inc. Total EGFR antibody was purchased from Bethyl Laboratories. The NF1 antibody was used as previously described (45).

Generation of Drug-Resistant Cell Lines

To generate drug-resistant cell lines, NSCLC cells were exposed to increasing concentrations of WZ4002 similar to previously described methods (12, 14, 32). Individual clones from WZR cells were isolated and confirmed to be drug resistant.

EGFR Mutational Analyses

Total RNA was isolated from cell lines or tumors using TRIzol (Invitrogen) and purified using RNeasy MinElute Cleanup Kit (Qiagen). cDNA was transcribed with Superscript II Reverse Transcriptase (Invitrogen Life Technologies) and used as template for subsequent

Published OnlineFirst September 7, 2012; DOI:10.1158/2159-8290.CD-12-0103

qRT-PCR–based studies (14, 32). The qRT-PCR products were also cloned into a TOPO TA vector (Invitrogen), transformed into bacteria, and the inserts from individual clones sequenced. The qRT-PCR primers and conditions are available upon request.

SNP Analyses

SNP analyses were conducted as previously described (14). Samples were processed for the Human Mapping 250K Sty single-nucleotide polymorphism (SNP) array according to the manufacturer's instructions. Comparison of gene copy number differences was conducted using the dChip software according to previously established methods (14, 46). The SNP data have been deposited to GEO (accession number GSE37700).

MAPK1 Copy Number Analysis

The absolute copy number for *MAPK1* was determined using qRT-PCR as previously described (14). Quantification was based on standard curves from a serial dilution of normal human genomic DNA. All specimens were analyzed in triplicate. The qRT-PCR primers are available upon request.

FISH Probes and Hybridization

The human *MAPK1* probe consisted of a mixture of 3 fosmids (WI2-1114H9, WI2-1468D5, and WI2-3011D5) and spanned the entire gene locus. A bacterial artificial chromosome (BAC; RP11-768L22) located on 22q13.33 was used as a reference probe. A BAC (RP24-174O22) was used as the murine *Mapk1* probe and BAC RP23-122A24 located on chromosome 16QA1 was used as a reference probe. All fosmids and BACS were purchased from Children's Hospital Oakland Research Institute. DNA was extracted using a Qiagen kit (Qiagen Inc.) and labeled with Spectrum Green– or Spectrum Orange–conjugated dUTP by nick translation (Vysis/Abbott Molecular). The CEP7 probe (Vysis/Abbott Molecular) was used according to the manufacturer's instructions. Chromosomal mapping and hybridization efficiency for each probe set were verified in normal metaphase spreads (data not shown). Three-color FISH assays were conducted as previously described (12, 14). Tumor cells were classified as containing a *MAPK1* amplification if the ratio of *MAPK1*/reference was 2 or more or if there were 1 or less reference signals and 3 or more *MAPK1* signals.

Generation of Mouse Cohorts and Treatment with WZ4002

Doxycycline inducible EGFR-TL (L858R/T790M) and EGFR-TD (Del E746_A750/T790M) transgenic mice were generated as previously described (13, 47). All mice were housed in a pathogen-free environment at the Harvard School of Public Health and were handled in strict accordance with Good Animal Practice as defined by the Office of Laboratory Animal Welfare, and all animal work was done with Dana-Farber Cancer Institute IACUC approval.

Cohorts of EGFR TL/CCSP-rtTA and EGFR TD/CCSP-rtTA were put on a doxycycline diet at 6 weeks of age to induce the expression of mutant *EGFR*. Mice were evaluated by MRI after 12 to 16 weeks of doxycycline diet to document and quantify the lung cancer burden before being assigned to various treatment study cohorts. Tumor-bearing mice were treated either with vehicle [NMP (10% 1-methyl-2-pyrrolidinone: 90% PEG-300)] alone or WZ4002 at 50 mg/kg gavage daily. Following the development of WZ4002 resistance, mice were treated with both WZ4002 (50 mg/kg daily oral gavage) and GSK-1120212 (1.5 mg/kg daily by oral gavage). MRI evaluation was repeated every 2 weeks. MRI and tumor burden measurement were conducted as described previously (47, 48).

MRI Scanning and Tumor Volume Measurement

Mice were anesthetized with 1% isoflurane in an oxygen/air mixture. The respiratory and cardiac rates of anesthetized mice were monitored using Biotrig Software. The animals were imaged with a rapid acquisition with relaxation enhancement sequence (TR = 2000 ms, TE effect = 25 ms) in the coronal and axial planes with a 1-mm slice thickness and with sufficient number of slices to cover the entire lung. A matrix size of 128×128 and a field of view of 2.5×2.5 cm^2 were used for all imaging. With the same geometry as described above, the mice were also imaged with a gradient echo fast imaging sequence (TR = 180 ms, TE effect = 2.2 ms) with respiratory and cardiac gating, in both the coronal and axial planes. The detailed procedure for MRI scanning has been previously described (47, 48). The tumor burden volume and quantification were reconstructed using 3-dimensional Slicer software (49).

Immunohistochemical Analyses

Hematoxylin and eosin (H&E) staining of tumor sections was conducted at the Department of Pathology at the Brigham and Women's Hospital. Immunohistochemistry for pEGFR and pERK1/2 was conducted on formalin-fixed paraffin-embedded tumor sections using previously described methods (13).

EGF Radiolabeling and Measurement of EGF Internalization Rate Constants

Recombinant human EGF (Peprotech) was labeled with ^{125}I (PerkinElmer) in the presence of an iodobead catalyst (Thermo Scientific) as described previously (50). The activity of the labeled EGF was determined using a phosphotungstic acid precipitation assay. To measure rate constants for labeled EGF internalization (k_e), serum-starved cells were exposed to 10 ng/mL ^{125}I-EGF at 37°C for up to 7.5 min. At 5 evenly spaced time points, cells were quickly washed with a buffer to remove bulk ligand, incubated in a mild acid strip solution to obtain surface-associated ligand, and finally solubilized in 1 N NaOH to obtain internalized ligand. Buffer washes and incubations were done at 4°C to minimize further EGFR internalization during these steps. ^{125}I-EGF counts in surface and internal fractions were quantified using a 1470 Wizard Gamma Counter (PerkinElmer). With these data, k_e values were calculated using a simple kinetic model of ligand-mediated receptor internalization, as described previously (50). Measurements were corrected for ^{125}I-EGF spillover from acid stripping and nonspecific binding of ^{125}I-EGF to the cell surface. For some measurements, cells were pretreated for approximately 24 hours with 3 μmol/L CI-1040.

RNA Expression Profiling and qRT-PCR

Total RNA was prepared from drug-sensitive and drug-resistant cells as described above. Synthesis of cRNA and hybridization to Human Expression Array U133A2.0 chips were conducted following Affymetrix protocols (Affymetrix, Inc.). Probe-level intensity data files in the .CEL format were preprocessed using Robust Multichip Average program using the Gene Pattern software (Broad Institute). Probes representing the same genes were collapsed into a single value, and standardized by taking the median value for each gene across sample set in the GenePattern software. Comparative maker selection module was used to select differentially expressed genes that meet defined criteria [$P < 0.0025$, fold change (FC) > 3.9]. Hierarchical clustering of the differentially expressed genes that met the criteria was conducted using GENE-E (Broad Institute). The expression data have been deposited to GEO (accession number GSE37700). To evaluate expression of genes associated with MEK/ERK-dependent transcriptional output, qRT-PCR was conducted in triplicate as described previously (24). NF1 expression was conducted using the NF1-TaqMan Gene Expression Assay (Mm00812424_m1; Applied Biosystems).

BH3 Profiling

BH3 profiling was conducted as previously described (31).

Published OnlineFirst September 7, 2012; DOI:10.1158/2159-8290.CD-12-0103

FACS Analyses

Cell viability experiments were conducted using drug-sensitive and drug-resistant cell lines exposed following drug exposure for 24 to 72 hours. Cells were stained with fluorescent conjugates of annexin-V (BioVision) and/or propidium iodide (PI) and analyzed on a FACS-Canto machine (Becton Dickinson). Viable cells are annexin-V and PI negative, and cell death is expressed as a percent of viable cells.

Patients

NSCLC patients treated with erlotinib were identified from the Thoracic Oncology Program at the Dana-Farber Cancer Institute. Tumor biopsies at the time of relapse were obtained under an IRB-approved protocol. Analyses for *EGFR* T790M and *MET* amplification were conducted as previously described (14). All patients provided written informed consent.

Disclosure of Potential Conflicts of Interest

P.A. Jänne is a consultant/advisory board member of AstraZeneca, Boehringer Ingelheim, Pfizer, Roche, Genentech, and Sanofi, has post-marketing royalties from Dana-Farber Cancer Institute–owned intellectual property on *EGFR* mutations licensed to Lab Corp, and is an inventor on a Dana-Farber Cancer Institute–owned patent on WZ4002.

A. Letai is a consultant/advisory board member of Eutropics Pharmaceuticals.

L. Garraway is a consultant/advisory board member and has a commercial research grant from Novartis Pharmaceuticals. L. Garraway also has ownership interest in Foundation Medicine.

N.S. Gray is an inventor on Dana-Farber Cancer Institute–owned patent on WZ4002 and has ownership interest (including patents)in Gatekeeper, Inc.

Neal Rosen has commercial research grants from AstraZeneca, Merck, and Chugai and is a consultant/advisory board member of Chugai, Astra-Zeneca, GSK, Novartis, and Millenium.

No potential conflicts of interest were disclosed by the other authors.

Authors' Contributions

Conception and design: D. Ercan, A. Letai, N.S. Gray, K.-K. Wong, P.A. Janne

Development of methodology: C. Xu, T. Shimamura, M. Capelletti

Acquisition of data (provided animals, acquired and managed patients, provided facilities, etc.): D. Ercan, C. Xu, M. Yanagita, C.S. Monast, C.A. Pratilas, J. Montero, M. Butaney, T. Shimamura, L. Sholl, A. Rogers, C. Repellin, M. Capelletti, O. Maertens, E.M. Goetz, M.J. Lazzara, N. Rosen, K.-K. Wong, P.A. Janne

Analysis and interpretation of data (e.g., statistical analysis, biostatistics, computational analysis): D. Ercan, C.S. Monast, C.A. Pratilas, J. Montero, M. Butaney, T. Shimamura, E.V. Ivanova, M. Tadi, A. Rogers, C. Repellin, M. Capelletti, A. Letai, M.J. Lazzara, N. Rosen, P.A. Janne

Writing, review, and/or revision of the manuscript: D. Ercan, C.S. Monast, M. Butaney, T. Shimamura, A. Rogers, C. Repellin, M.J. Lazzara, N. Rosen, K.-K. Wong, P.A. Janne

Administrative, technical, or material support (i.e., reporting or organizing data, constructing databases): M. Yanagita, M. Tadi, L.A. Garraway, M.J. Lazzara, P.A. Janne

Study supervision: N.S. Gray, P.A. Janne

Acknowledgments

This study is supported by grants from NIH R01CA114465 (P.A. Janne), R01CA135257 (P.A. Janne), P01CA154303 (P.A. Janne, K.-K. Wong, and N.S. Gray), K08CA127350 (C.A. Pratilas), National Cancer Institute Lung SPORE P50CA090578 (P.A. Janne and K.-K. Wong), the Cammarata Family Foundation Research Fund (M. Capelletti and P.A. Janne), the Nirenberg Fellowship at Dana-Farber Cancer Institute (M. Capelletti and P.A. Janne), and the American Cancer Society IRG-78-002-30 (M.J. Lazzara and C.S. Monast).

Received March 9, 2012; revised August 3, 2012; accepted August 7, 2012; published OnlineFirst September 7, 2012.

REFERENCES

1. Rosell R, Carcereny E, Gervais R, Vergnenegre A, Massuti B, Felip E, et al. Erlotinib versus standard chemotherapy as first-line treatment for European patients with advanced EGFR mutation-positive non-small-cell lung cancer (EURTAC): a multicentre, open-label, randomised phase 3 trial. Lancet Oncol 2012;13:239–46.
2. Zhou C, Wu YL, Chen G, Feng J, Liu XQ, Wang C, et al. Erlotinib versus chemotherapy as first-line treatment for patients with advanced EGFR mutation-positive non-small-cell lung cancer (OPTIMAL, CTONG-0802): a multicentre, open-label, randomised, phase 3 study. Lancet Oncol 2011;12:735–42.
3. Mok TS, Wu YL, Thongprasert S, Yang CH, Chu DT, Saijo N, et al. Gefitinib or carboplatin-paclitaxel in pulmonary adenocarcinoma. N Engl J Med 2009;361:947–57.
4. Engelman JA, Janne PA. Mechanisms of acquired resistance to epidermal growth factor receptor tyrosine kinase inhibitors in non-small cell lung cancer. Clin Cancer Res 2008;14:2895–9.
5. Kobayashi S, Boggon TJ, Dayaram T, Janne PA, Kocher O, Meyerson M, et al. EGFR mutation and resistance of non-small-cell lung cancer to gefitinib. N Engl J Med 2005;352:786–92.
6. Pao W, Miller VA, Politi KA, Riely GJ, Somwar R, Zakowski MF, et al. Acquired resistance of lung adenocarcinomas to gefitinib or erlotinib is associated with a second mutation in the EGFR kinase domain. PLoS Med 2005;2:1–11.
7. Sequist LV, Waltman BA, Dias-Santagata D, Digumarthy S, Turke AB, Fidias P, et al. Genotypic and histological evolution of lung cancers acquiring resistance to EGFR inhibitors. Sci Transl Med 2011;3:75ra26.
8. Yun CH, Mengwasser KE, Toms AV, Woo MS, Greulich H, Wong KK, et al. The T790M mutation in EGFR kinase causes drug resistance by increasing the affinity for ATP. Proc Natl Acad Sci U S A 2008;105:2070–5.
9. Li D, Ambrogio L, Shimamura T, Kubo S, Takahashi M, Chirieac LR, et al. BIBW2992, an irreversible EGFR/HER2 inhibitor highly effective in preclinical lung cancer models. Oncogene 2008;27:4702–11.
10. Engelman JA, Zejnullahu K, Gale CM, Lifshits E, Gonzales AJ, Shimamura T, et al. PF00299804, an irreversible pan-ERBB inhibitor, is effective in lung cancer models with EGFR and ERBB2 mutations that are resistant to gefitinib. Cancer Res 2007;67:11924–32.
11. Miller VA, Hirsh V, Cadranel J, Chen Y-M, Park K, Kim S-W, et al. Phase IIB/III double-blind randomized trial of afatinib (BIBW2992, an irreversible inhibitor of EGFR/HER1 and HER2) + best supportive care (BSC) versus placebo + BSC in patients with NSCLC failing 1–2 lines of chemotherapy and erlotinib or gefitinib (LUX-LUNG 1). Ann Oncol 2010;21:LBA1.
12. Ercan D, Zejnullahu K, Yonesaka K, Xiao Y, Capelletti M, Rogers A, et al. Amplification of EGFR T790M causes resistance to an irreversible EGFR inhibitor. Oncogene 2010;29:2346–56.
13. Zhou W, Ercan D, Chen L, Yun CH, Li D, Capelletti M, et al. Novel mutant-selective EGFR kinase inhibitors against EGFR T790M. Nature 2009;462:1070–4.
14. Engelman JA, Zejnullahu K, Mitsudomi T, Song Y, Hyland C, Park JO, et al. MET amplification leads to gefitinib resistance in lung cancer by activating ERBB3 signaling. Science 2007;316:1039–43.
15. Aronov AM, Tang Q, Martinez-Botella G, Bemis GW, Cao J, Chen G, et al. Structure-guided design of potent and selective pyrimidylpyrrole inhibitors of extracellular signal-regulated kinase (ERK) using conformational control. J Med Chem 2009;52:6362–8.
16. Dalby KN, Morrice N, Caudwell FB, Avruch J, Cohen P. Identification of regulatory phosphorylation sites in mitogen-activated protein kinase (MAPK)-activated protein kinase-1a/p90rsk that are inducible by MAPK. J Biol Chem 1998;273:1496–505.

Published OnlineFirst September 7, 2012; DOI:10.1158/2159-8290.CD-12-0103

17. Raynaud FI, Eccles S, Clarke PA, Hayes A, Nutley B, Alix S, et al. Pharmacologic characterization of a potent inhibitor of class I phosphatidylinositide 3-kinases. Cancer Res 2007;67:5840–50.
18. Tan S, Ng Y, James DE. Next-generation Akt inhibitors provide greater specificity: effects on glucose metabolism in adipocytes. Biochem J 2011;435:539–44.
19. Marks JL, Gong Y, Chitale D, Golas B, McLellan MD, Kasai Y, et al. Novel MEK1 mutation identified by mutational analysis of epidermal growth factor receptor signaling pathway genes in lung adenocarcinoma. Cancer Res 2008;68:5524–8.
20. Costa DB, Halmos B, Kumar A, Schumer ST, Huberman MS, Boggon TJ, et al. BIM mediates EGFR tyrosine kinase inhibitor-induced apoptosis in lung cancers with oncogenic EGFR mutations. PLoS Med 2007;4:1669–79; discussion 80.
21. Deng J, Shimamura T, Perera S, Carlson NE, Cai D, Shapiro GI, et al. Proapoptotic BH3-only BCL-2 family protein BIM connects death signaling from epidermal growth factor receptor inhibition to the mitochondrion. Cancer Res 2007;67:11867–75.
22. Gong Y, Somwar R, Politi K, Balak M, Chmielecki J, Jiang X, et al. Induction of BIM is essential for apoptosis triggered by EGFR kinase inhibitors in mutant EGFR-dependent lung adenocarcinomas. PLoS Med 2007;4:e294.
23. Jeffrey KL, Camps M, Rommel C, Mackay CR. Targeting dual-specificity phosphatases: manipulating MAP kinase signalling and immune responses. Nat Rev Drug Discov 2007;6:391–403.
24. Pratilas CA, Taylor BS, Ye Q, Viale A, Sander C, Solit DB, et al. (V600E)BRAF is associated with disabled feedback inhibition of RAF-MEK signaling and elevated transcriptional output of the pathway. Proc Natl Acad Sci U S A 2009;106:4519–24.
25. Owens DM, Keyse SM. Differential regulation of MAP kinase signalling by dual-specificity protein phosphatases. Oncogene 2007;26:3203–13.
26. Kim HJ, Bar-Sagi D. Modulation of signalling by Sprouty: a developing story. Nat Rev Mol Cell Biol 2004;5:441–50.
27. Schubbert S, Shannon K, Bollag G. Hyperactive Ras in developmental disorders and cancer. Nat Rev Cancer 2007;7:295–308.
28. Li X, Huang Y, Jiang J, Frank SJ. ERK-dependent threonine phosphorylation of EGF receptor modulates receptor downregulation and signaling. Cell Signal 2008;20:2145–55.
29. Takishima K, Griswold-Prenner I, Ingebritsen T, Rosner MR. Epidermal growth factor (EGF) receptor T669 peptide kinase from 3T3-L1 cells is an EGF-stimulated "MAP" kinase. Proc Natl Acad Sci U S A 1991;88:2520–4.
30. Northwood IC, Gonzalez FA, Wartmann M, Raden DL, Davis RJ. Isolation and characterization of two growth factor-stimulated protein kinases that phosphorylate the epidermal growth factor receptor at threonine 669. J Biol Chem 1991;266:15266–76.
31. Ni Chonghaile T, Sarosiek KA, Vo TT, Ryan JA, Tammareddi A, Moore Vdel G, et al. Pretreatment mitochondrial priming correlates with clinical response to cytotoxic chemotherapy. Science 2011;334:1129–33.
32. Engelman JA, Mukohara T, Zejnullahu K, Lifshits E, Borras AM, Gale CM, et al. Allelic dilution obscures detection of a biologically significant resistance mutation in EGFR-amplified lung cancer. J Clin Invest 2006;116:2695–706.
33. Engelman JA, Janne PA, Mermel C, Pearlberg J, Mukohara T, Fleet C, et al. ErbB-3 mediates phosphoinositide 3-kinase activity in gefitinib-sensitive non-small cell lung cancer cell lines. Proc Natl Acad Sci U S A 2005;102:3788–93.
34. Turke AB, Zejnullahu K, Wu YL, Song Y, Dias-Santagata D, Lifshits E, et al. Preexistence and clonal selection of MET amplification in EGFR mutant NSCLC. Cancer Cell 2010;17:77–88.
35. Donev IS, Wang W, Yamada T, Li Q, Takeuchi S, Matsumoto K, et al. Transient PI3K inhibition induces apoptosis and overcomes HGF-mediated resistance to EGFR-TKIs in EGFR mutant lung cancer. Clin Cancer Res 2011;17:2260–9.
36. Maheswaran S, Sequist LV, Nagrath S, Ulkus L, Brannigan B, Collura CV, et al. Detection of mutations in EGFR in circulating lung-cancer cells. N Engl J Med 2008;359:366–77.
37. Ogino A, Kitao H, Hirano S, Uchida A, Ishiai M, Kozuki T, et al. Emergence of epidermal growth factor receptor T790M mutation during chronic exposure to gefitinib in a non small cell lung cancer cell line. Cancer Res 2007;67:7807–14.
38. Chmielecki J, Foo J, Oxnard GR, Hutchinson K, Ohashi K, Somwar R, et al. Optimization of dosing for EGFR-mutant non-small cell lung cancer with evolutionary cancer modeling. Sci Transl Med 2011;3: 90ra59.
39. Godin-Heymann N, Ulkus L, Brannigan BW, McDermott U, Lamb J, Maheswaran S, et al. The T790M "gatekeeper" mutation in EGFR mediates resistance to low concentrations of an irreversible EGFR inhibitor. Mol Cancer Ther 2008;7:874–9.
40. Lazzara MJ, Lane K, Chan R, Jasper PJ, Yaffe MB, Sorger PK, et al. Impaired SHP2-mediated extracellular signal-regulated kinase activation contributes to gefitinib sensitivity of lung cancer cells with epidermal growth factor receptor-activating mutations. Cancer Res 2010;70:3843–50.
41. Ono M, Hirata A, Kometani T, Miyagawa M, Ueda S, Kinoshita H, et al. Sensitivity to gefitinib (Iressa, ZD1839) in non-small cell lung cancer cell lines correlates with dependence on the epidermal growth factor (EGF) receptor/extracellular signal-regulated kinase 1/2 and EGF receptor/Akt pathway for proliferation. Mol Cancer Ther 2004;3:465–72.
42. Gilmartin AG, Bleam MR, Groy A, Moss KG, Minthorn EA, Kulkarni SG, et al. GSK1120212 (JTP-74057) is an inhibitor of MEK activity and activation with favorable pharmacokinetic properties for sustained *in vivo* pathway inhibition. Clin Cancer Res 2011;17:989–1000.
43. Paez JG, Janne PA, Lee JC, Tracy S, Greulich H, Gabriel S, et al. EGFR mutations in lung cancer: correlation with clinical response to gefitinib therapy. Science 2004;304:1497–500.
44. Mukohara T, Engelman JA, Hanna NH, Yeap BY, Kobayashi S, Lindeman N, et al. Differential effects of gefitinib and cetuximab on non-small-cell lung cancers bearing epidermal growth factor receptor mutations. J Natl Cancer Inst 2005;97:1185–94.
45. McGillicuddy LT, Fromm JA, Hollstein PE, Kubek S, Beroukhim R, De Raedt T, et al. Proteasomal and genetic inactivation of the NF1 tumor suppressor in gliomagenesis. Cancer Cell 2009;16:44–54.
46. Zhao X, Weir BA, LaFramboise T, Lin M, Beroukhim R, Garraway L, et al. Homozygous deletions and chromosome amplifications in human lung carcinomas revealed by single nucleotide polymorphism array analysis. Cancer Res 2005;65:5561–70.
47. Li D, Shimamura T, Ji H, Chen L, Haringsma HJ, McNamara K, et al. Bronchial and peripheral murine lung carcinomas induced by T790M-L858R mutant EGFR respond to HKI-272 and rapamycin combination therapy. Cancer Cell 2007;12:81–93.
48. Ji H, Li D, Chen L, Shimamura T, Kobayashi S, McNamara K, et al. The impact of human EGFR kinase domain mutations on lung tumorigenesis and *in vivo* sensitivity to EGFR-targeted therapies. Cancer Cell 2006;9:485–95.
49. 3D Slicer [homepage on the Internet]. Boston: Brigham and Women's Hospital; c2012 [cited 2012 Aug 3]. Available from: http://www.slicer.org/.
50. Lund KA, Opresko LK, Starbuck C, Walsh BJ, Wiley HS. Quantitative analysis of the endocytic system involved in hormone-induced receptor internalization. J Biol Chem 1990;265:15713–23.